Crystal Effects in the Neutralization of He^+ Ions in the Low Energy Ion Scattering Regime

D. Primetzhofer,[1] S. N. Markin,[1] J. I. Juaristi,[2] E. Taglauer,[3] and P. Bauer[1,*]

[1]*Institut für Experimentalphysik, Johannes Kepler Universität Linz, A-4040 Linz, Austria*
[2]*Departamento de Fisica de Materiales, Facultad de Ciencias Quimicas, Apartado 1072, E-20080 San Sebastian, Spain*
[3]*Max-Planck-Institutfür Plasmaphysik, EURATOM Association, D-85748 Garching bei München, Germany*

(Received 26 March 2007; revised manuscript received 19 October 2007; published 28 May 2008)

Investigating possible crystal effects in ion scattering from elemental surfaces, measurements of the positive ion fraction P^+ are reported for He^+ ions scattered from single and polycrystalline Cu surfaces. In the Auger neutralization regime, the ion yield is determined by scattering from the outermost atomic layer. For Cu(110) P^+ exceeds that for polycrystalline Cu by up to a factor of 2.5, thus exhibiting a strong crystal effect. It is much less pronounced at higher energies, i.e., in the reionization regime. However, there a completely different angular dependence of the ion yield is observed for poly- and single crystals, due to massive subsurface contributions in nonchanneling directions.

DOI: 10.1103/PhysRevLett.100.213201 PACS numbers: 34.35.+a, 68.47.De, 68.49.Sf, 79.20.Rf

In low-energy ion scattering (LEIS) neutralization of the primary ions during the scattering process is a decisive physical phenomenon. Backscattered ions originate mainly from collisions with top layer atoms. Thus, neutralization makes LEIS a very surface sensitive analysis method. However, although the charge transfer mechanisms are known and qualitatively well understood, a quantitative prediction of the scattered ion yield is generally not possible. Nevertheless, appropriate calibration by use of elemental standards is quite frequently possible and therefore many investigations achieving not only qualitative but also quantitative surface composition analysis are reported in the literature. The situation is well documented in a very recent review [1].

Calibration procedures often rely on the experience that in LEIS matrix effects are absent or at least negligible. This means that for the backscattered projectiles the final charge state distribution depends only on the species of projectile and scattering center, irrespective of the chemical environment of the scattering atom. Influence of other surface atoms on the ion yield has, however, been reported in cases of so-called ''trajectory dependent neutralization'' [2–5]. This is particularly so in cases in which resonant charge transfer is effective.

Here we report for the first time on the observation of strong crystal effects for scattering of He^+ ions from an elemental surface, i.e., single and polycrystalline Cu. The results are explained within the concepts of Auger neutralization (AN) and collision induced ionization and neutralization (CIR, CIN), which for noble gas ions represent the dominant charge exchange processes, and by taking the influence of the crystal structure into account. Possible consequences on surface composition analysis by LEIS are discussed on this basis.

Auger neutralization along the trajectory is possible at any primary energy [6]. The neutralization rate $-dP^+/dt$ depends on the Auger transition rate Γ_A via $-dP^+/dt = P^+\Gamma_A$. From this, the surviving probabilities ${P^+}_{\text{in}}$ and ${P^+}_{\text{out}}$ for incoming and outgoing trajectories are obtained as

$$
\begin{aligned}
{P^+}_j &= \exp\left[-\int_0^{\Delta t_j}\Gamma_A(z(t))dt\right] = \exp[-\langle\Gamma_A\rangle\Delta t_j] \\
&\approx \exp[-\langle\Gamma_A\rangle\Delta z_j/V_{\perp j}] \equiv \exp[-V_{cj}/V_{\perp j}], \qquad (1)
\end{aligned}
$$

where j stands for *in* or *out*, $\langle\Gamma_A\rangle$ denotes the transition rate averaged over the trajectory and Δt is the time spent by the projectile in the region, where neutralization takes place, i.e., with a high density of conduction electrons. In Eq. (1) also the characteristic velocity V_c is defined as a measure of neutralization efficiency. From Eq. (1) it is clear that AN scales approximately with the normal component $V_\perp$ of the projectile velocity. The fraction ${P_{\text{AN}}}^+$ of projectiles that has survived surface scattering without being neutralized by AN is given by ${P_{\text{AN}}}^+ = {P^+}_{\text{in}} \cdot {P^+}_{\text{out}} = \exp[-\langle\Gamma_A\rangle \times (\Delta t_{\text{in}} + \Delta t_{\text{out}})] \approx \exp(-V_c/V_\perp)$, with the abbreviation $1/V_\perp \equiv 1/V_{\perp\text{in}} + 1/V_{\perp\text{out}}$.

In the ''reionization regime'', *collision induced processes*, CIN and CIR, become possible at distances smaller than a critical value $R_{\min}(E, \theta)$ due to the evolution of molecular orbitals [7–9]. In the collision between the projectile and a target atom, a minimum distance smaller than $R_{\min}$ is reached if—for a fixed scattering angle θ—the projectile energy E is larger than a certain threshold E_{th}. The specific value of E_{th} depends on the atomic species of the collision partners and on the scattering angle θ; e.g., for He^+ and Cu and $\theta = 129°$, $E_{\text{th}} = 2100$ eV [1]. For $E > E_{\text{th}}$, P^+ is therefore not a unique function of $V_\perp$, since for a given projectile—target atom combination the probabilities for the collision induced processes, P_{CIN} and P_{CIR}, depend on E and θ instead of $V_\perp$. Consequently, for given values of $V_\perp$ and θ, P^+ is a double valued function, depending on α and β, with an apex at $\alpha \approx \beta$ [10]; α and β are measured with respect to the surface normal.

Thus, for backscattering from surface atoms at $E > E_{\text{th}}$, the ion fraction is obtained as the sum of two contributions,

i.e., survivals and reionized projectiles [11]:

$$P^+ = P^+_{\text{in}}(1 - P_{\text{CIN}})P^+_{\text{out}} + (1 - P^+_{\text{in}})P_{\text{CIR}}P^+_{\text{out}}. \quad (2)$$

In the present study we focus on charge exchange of He^+ ions on nonequivalent Cu single crystal surfaces, i.e., Cu(100), Cu(110), and polycrystalline Cu [12]. Thus, we keep electronic configuration ($3d^{10}4s^1$) and crystal structure (fcc) constant, and study charge exchange at surfaces with different atomic configurations and correspondingly different electronic properties. The experiment was performed using the TOF-LEIS setup ACOLISSA [13], where the samples are mounted on a 5 axes manipulator, permitting three translations and two rotations (angle of incidence α and azimuth φ). Polished crystals were purchased with a roughness below 0.03 μm and a precision of the orientation of $\pm 0.1°$; the surfaces were prepared by cycles of 3 keV Ar^+-sputtering and annealing to $\geq 400\,°C$. Auger electron spectroscopy (AES) did not show any impurities after cleaning, in low-energy electron diffraction (LEED) sharp spots were observed, indicating good crystal quality. TOF-LEIS measurements were performed in the energy range 0.8 to 10 keV. Particles scattered by $\theta = 129°$ were analyzed, the resulting ion and neutral TOF spectra were recorded for a given scattering geometry, i.e., for specific values for α and φ.

In double alignment geometry, backscattering from subsurface layers is very efficiently inhibited since the incident beam is directed towards the crystal along a low index direction (channelling). That is, the atoms in deeper layers are in the ''shadow'' of the top layer atoms. Similarly, the outgoing projectiles leave the sample in a low index direction towards the detector, again blocking deeper layer atoms [14]. Under these conditions, single scattering is limited to surface layer atoms. The corresponding ion fraction was deduced from the rather well-defined areas in the TOF- spectra of the ion peak and of the surface peak of the neutrals [15], A_+ and A_0, respectively, (see Fig. 1) taking detection efficiencies into account [1]. By doing so subsurface contributions are very efficiently eliminated, and the surface peak intensities in double alignment geometry are almost exclusively due to single scattering for both, ions and neutrals [1]. For all other angles, $P^+(\alpha)$ was obtained from $P^+(\alpha = 0)$ via $A_+(\alpha)$ and $A_+(\alpha = 0)$, measured for the identical number of primary projectiles (see Fig. 1). Similarly, P^+_{poly} was obtained by comparing the ion yields for the polycrystal and Cu(100), again for the identical number of primary projectiles, taking the different atomic surface densities into account.

The selection of He^+ and Cu permits to explore neutralization exclusively due to AN in a wide energy range, i.e., for $E < E_{\text{th}} = 2100$ eV [10,16]. In this regime polar scans ($-15° \leq \alpha \leq 70°$, with respect to the surface normal) were performed for Cu(100) along the [001] azimuth, for Cu(110) along the $[1\bar{1}2]$ azimuth, and for polycrystalline Cu. The results are shown in Fig. 2 in a semi logarithmic plot of P^+ as a function of $1/V_\perp$. For each of the Cu surfaces, the P^+ data are very well described by a single

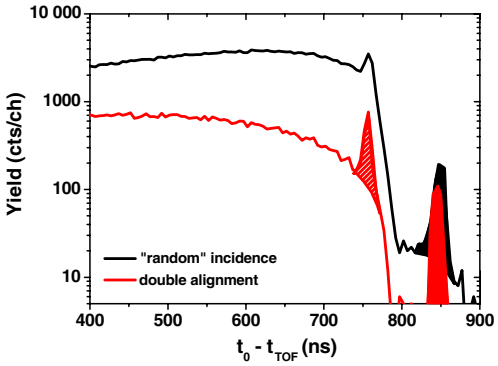

FIG. 1 (color online). Experimental spectra are shown as a function of the inverse time-of-flight $t_0 - t_{\text{TOF}}$, where t_0 is a constant and t_{TOF} the time-of-flight for 5 keV He^+ ions and a Cu(100) surface. The spectra refer to double alignment geometry [$\alpha = 0°$, $\beta = 51°$, azimuth in (001) direction, gray line (red online)]; and to ''random'' geometry ($\alpha = 25°$, $\beta = 26°$, azimuth in (001) direction, black line). The surface peak intensities of ions and neutrals after subtraction of a linear background are indicated as hatched and filled areas, respectively.

exponential function, as predicted by Eq. (1). Thus, the $V_\perp$ scaling of P^+ in the AN regime is perfectly fulfilled within statistical uncertainties ($\pm$ 7% per data point).

For the single crystals the azimuth directions were chosen such that each polar scan contains scattering geometries where double alignment conditions are fulfilled for $\alpha = 0°$ and $\alpha = 51°$. As may be seen in Fig. 2, double alignment does not yield any noticeable influence on the ion fraction. From this it may be concluded that in the AN regime the information depth is limited to the outermost atomic layer in any case—even in random geometry, as a consequence of the high neutralization efficiency of AN.

When comparing P^+ for different Cu surfaces, large systematic differences are observed (see Fig. 2), with largest P^+ values for Cu(110) ($P^+_{(110)}$) and lowest for polycrystalline Cu (P^+_{poly}). For instance, at $1/V_\perp =$

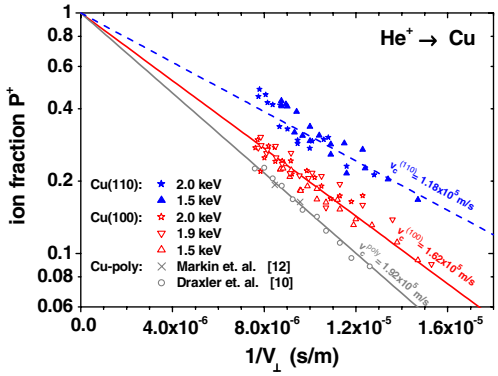

FIG. 2 (color online). Ion fraction P^+ of He^+ scattered from Cu(110) (full symbols), Cu(100) (open asterisks and triangles) and polycrystalline Cu (crosses and open circles) in the AN regime, as a function of $1/V_\perp = 1/V_{\perp\text{in}} + 1/V_{\perp\text{out}}$. Also shown are single exponential fits [see Eq. (1)] with characteristic velocity values as indicated in the figure (for details see text).

1.25×10^{-5} s/m, $P^+_{(110)}$ exceeds P^+_{poly} by a factor of ~2.5. This represents a pronounced crystal effect, just as a consequence of different surface structures for a pure element. This is striking on the basis that LEIS is a quantitative surface analytical tool. To understand qualitatively the origin of this crystal effect, it is illustrative to deduce a mean Auger transition rate for each of the data sets shown in Fig. 2. By limiting neutralization to distances smaller than half an interlayer distance [17,18], one can calculate the time spent by the projectile within the electron cloud when being backscattered from a surface atom. This was done by molecular dynamics simulations (KALYPSO [19]). As a result, for both single crystal surfaces, one common mean AN rate $\langle \Gamma_A \rangle = (2.17 \pm 0.02) \times 10^{15}$ s^{-1} is obtained. One can therefore conclude that the observed crystal effect is just a consequence of the fact that the time available for neutralization depends on the specific orientation of the crystal surface. Consequently, the commonly used way to characterize P^+ in the AN regime via the characteristic velocity V_c is inadequate; it is more appropriate to describe AN via $P^+_j \approx \exp[-\langle \Gamma_A \rangle \Delta z_j / V_{\perp j}]$ [see Eq. (1)]. Note that the same Auger rate is obtained also for the polycrystal assuming it to consist of (111) facets. These results are corroborated by the fact that also for Al(110) and Al(111) surfaces one can derive one common value $\langle \Gamma_{A,Al} \rangle = 5.8 \times 10^{14}$ s^{-1} from z-dependent Auger rates deduced from LCAO calculations [18]. The fact that the Auger rate is lower for Al than for Cu, indicates that in the latter case also the d-electrons contribute considerably to AN [20].

Figure 2 shows that this crystal effect decreases with increasing energy. From that observation one might expect that the high energy regime may be more suitable in the face of quantitative analysis. To further explore this we also performed polar scans for Cu(100) and Cu(110) at energies $E > E_{th}$. Data recording and analysis were performed in a similar way as in the low-energy regime, taking advantage of the double alignment geometries. In Fig. 3(a), a typical P^+ result obtained for Cu(100) from a polar scan at $E = 6$ keV is shown together with the corresponding AN data, taken from Fig. 2. From Fig. 3(a) it is obvious that in the reionization regime the general behavior of P^+ is completely different from the AN regime: P^+ now is a double valued function of $1/V_\perp$, as expected—but is completely different from the boomeranglike shape as observed for P^+_{poly} in the reionization regime [10], and Eq. (2) is not sufficient to describe the observations.

A remarkable feature of the data shown in Fig. 3(a) is that the resulting P^+ values are virtually identical for double alignment conditions, i.e., for $\alpha \approx 0°$ and $\alpha \approx 51°$ [full symbols in Fig. 3(a)]. Outside double alignment conditions, a strong increase of the ion yield is observed for single crystals. This is shown in Fig. 3(a), where at the smallest $1/V_\perp$ value, corresponding to $\alpha = 25°$, i.e., at 4.3×10^{-6} s/m, the apparent P^+ exceeds the minimum value $P^+(\alpha = 0°)$ by a factor of ~3.

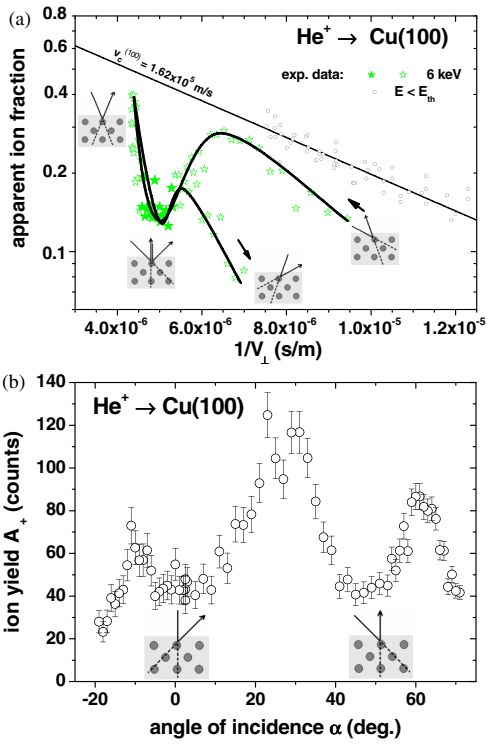

FIG. 3 (color online). (a) Apparent ion fraction P^+ of 6 keV He^+ scattered from Cu(100), as a function of $1/V_\perp = 1/V_{\perp in} + 1/V_{\perp out}$. Full asterisks refer to double alignment geometry, open asterisks to scattering out of double alignment. The corresponding scattering geometries are shown as inserts. For comparison, also the experimental results and the single exponential fit in the AN regime are shown (circles and full line, respectively, from Fig. 1). (b) Normalized ion yield A^+ as a function of the angle of incidence α for the identical data set presented in Fig. 2(a), for 6 keV He^+ scattered from Cu(100).

Obviously, for scattering from the outermost atomic layer, as in double alignment conditions, $P^+(1/V_\perp)$ is almost independent of α. This finding is compatible with the fact that for $E = 6$ keV AN is already rather ineffective such that the relative difference between $P^+_{out}(\beta)$ and $P^+_{out}(\beta = 0)$ is small, and collision induced processes are dominant.

The observed maximum in P^+ is caused by focussing collision cascades which direct a major part of the primary flux unto atoms in deeper layers leading to an increase of available scattering centers in subsurface layers and consequently of backscattered projectiles. This enhancement of backscattered intensity and its interplay with CIR and ineffective AN leads to the observed increase in P^+ due to reionization in a final large angle scattering process that may occur in or close to the surface [1]. This interpretation becomes more obvious when plotting the data as a function of α instead of $1/V_\perp$ [see Fig. 3(b)].

In Fig. 3(b), the minima at $\alpha = 0°$ and at 51° can easily be recognized as channelling dips found exactly at the expected angular position for the investigated system. The ion yield maximum at $\alpha = 25°$ corresponds to "random conditions", where focusing on deeper layer atoms is

of importance. In fact, away from double alignment the neutral yield is even more strongly enhanced than the ion yield. MARLOWE simulations revealed that—due to multiple scattering up to 10 crystal layers contribute to the measured scattering yield even at the final energy that corresponds to single scattering from atoms in the surface layer [15]. Consequently, the data in Fig. 3(a) represent only an apparent ion fraction since in any standard evaluation the unknown number of scattering centers for random single crystal orientation cannot be accounted for, but nevertheless a strong increase in the ion yield is observed.

These findings also shed light on the interpretation of polycrystal data for $E > E_{\mathrm{th}}$. For polycrystals, the angular dependence of $P^{+}(\alpha)$ observed at $E > E_{\mathrm{th}}$ is a consequence of three factors: first, the before mentioned strong subsurface contributions are also relevant for polycrystals; second, a final reionizing collision near to the surface converts neutrals to ions, and third, these reionized projectiles lead to the boomeranglike shape since they can escape AN on their way out for normal exit with higher probability.

Similar results as for Cu(100) were obtained for Cu(110), (not shown here) and analogous crystal effects were found. The resulting P^{+} data measured in double alignment are very close to the results for Cu(100), both in shape and in magnitude: for 6 keV He^{+} and perpendicular incidence, $P^{+}{}_{(110)} = 0.12$, and $P^{+}{}_{\mathrm{poly}} = 0.105$ is found.

We stress the point that the nature of the observed crystal effect [10] at energies larger than E_{th} is completely different from the findings in the AN regime since it is not related to the electronic but to the crystal structure of the sample.

Finally, we want to discuss the consequences of our findings for the reliability of quantitative surface composition analysis by LEIS. Experiments can be performed either in the AN regime or the reionization regime. Whatever choice is taken, one is left with different advantages and possible pitfalls. The main advantage of the *AN regime* is that the information depth is almost exclusively limited to the outermost atomic layer. However, there strong crystal effects have to be expected, depending on the crystal structure of the sample: for different Cu crystal faces, we report ion yields that differ by up to a factor of 2.5. Consequently, the characteristic velocity $V_c = \int_0^{\infty} \Gamma_A dz$ is not an appropriate measure to describe the efficiency of AN. More adequate is to use the quantity $V_{c,hkl} = \langle \Gamma_A \rangle \Delta z_{hkl}$ to account for the surface specific extension of the electron density in front of the surface. By appropriate selection of standard samples and scattering geometries, quantitative analysis may still be possible if these results are taken into account [21]. In the *reionization regime*, the dependence of P^{+} on the surface orientation is reduced due to the atomic character of collision induced processes and to inefficient AN. However, the scattering geometry has to be chosen carefully to limit the information depth to the outermost atomic layers—which is, however, not achievable for polycrystalline targets. To obtain a more complete understanding of the charge exchange in ion—surface scattering, a thorough theoretical description of this rather complex situation is required.

This work was partially supported by the Austrian Science Fund FWF, project number P16469. Inspiring discussions with P. Zeppenfeld and M. Draxler are acknowledged.

*Corresponding author.
peter.bauer@jku.at

[1] H. H. Brongersma, M. Draxler, M. de Ridder, and P. Bauer, Surf. Sci. Rep. **62**, 63 (2007).
[2] D. J. Godfrey and D. P. Woodruff, Surf. Sci. **105**, 438 (1981).
[3] D. J. Godfrey and D. P. Woodruff, Surf. Sci. **105**, 459 (1981).
[4] E. Taglauer, W. Englert, W. Heiland, and D. P. Jackson, Phys. Rev. Lett. **45**, 740 (1980).
[5] M. Beckschulte and E. Taglauer, Nucl. Instrum. Methods Phys. Res., Sect. B **78**, 29 (1993).
[6] H. D. Hagstrum, Phys. Rev. **96**, 336 (1954).
[7] R. Souda, M. Aono, C. Oshima, S. Otani, and Y. Ishizawa, Surf. Sci. **150**, L59 (1985).
[8] T. M. Thomas, H. Neumann, A. W. Czanderna, and J. R. Pitts, Surf. Sci. **175**, L737 (1986).
[9] N. P. Wang, E. A. Garcia, R. Monreal, F. Flores, E. C. Goldberg, H. H. Brongersma, and P. Bauer, Phys. Rev. A **64**, 012901 (2001).
[10] M. Draxler, R. Gruber, H. H. Brongersma, and P. Bauer, Phys. Rev. Lett. **89**, 263201 (2002).
[11] L. K. Verhey, B. Poelsema, and A. L. Boers, Nucl. Instrum. Methods **132**, 565 (1976).
[12] S. N. Markin, D. Primetzhofer, J. E. Valdés, E. Taglauer, and P. Bauer, Nucl. Instrum. Methods Phys. Res., Sect. B **258**, 18 (2007).
[13] M. Draxler, S. N. Markin, S. N. Ermolov, K. Schmid, C. Hesch, R. Gruber, A. Poschacher, M. Bergsmann, and P. Bauer, Vacuum **73**, 39 (2004).
[14] M. L. Swanson, in *Handbook of Modern Ion Beam Materials Analysis*, edited by J. R. Tesmer and M. Nastasi (Materials Research Society, Pittsburgh, PA, 1995), p. 231.
[15] D. Primetzhofer, S. N. Markin, J. E Valdés, E. Taglauer, R. Beikler, and P. Bauer, Nucl. Instrum. Methods Phys. Res., Sect. B **258**, 36 (2007).
[16] M. Aono and R. Souda, Nucl. Instrum. Methods Phys. Res., Sect. B **27**, 55 (1987).
[17] P. J. Jennings, R. O. Jones, and M. Weinert, Phys. Rev. B **37**, 6113 (1988).
[18] D. Valdés, E. C. Goldberg, J. M. Blanco, and R. C. Monreal, Phys. Rev. B **71**, 245417 (2005).
[19] M. A. Karolewski, Nucl. Instrum. Methods Phys. Res., Sect. B **230**, 402 (2005).
[20] D. Valdés, J. M. Blanco, V. A. Esaulov, and R. C. Monreal, Phys. Rev. Lett. **97**, 047601 (2006).
[21] A. Steltenpohl, N. Memmel, E. Taglauer, Th. Fauster, and J. Onsgaard, Surf. Sci. **382**, 300 (1997).